



Imprints of Modified Gravity Scenarios on the Inner Structure of Massive Dark Matter Halos



Pier Stefano Corasaniti

LUTH, CNRS and Observatoire de Paris

Modified Gravity

Modified Einstein-Hilbert Action

$$S = \int d^4x \sqrt{-g} \frac{R + f(R)}{16\pi G}$$

- Departure from GR as source of cosmic acceleration

- Reproduces observed cosmic expansion
- Observationally viable

- Screening mechanism recovers GR at small scales



- Imprints on Cosmic Structures

- Growth linear scales
- Screening effects & non-linear regime

Screening Mechanism

Einstein Frame

$$S = \int d^4x \sqrt{-g} \left[\frac{R}{16\pi G} - \frac{1}{2} \nabla_\mu \varphi \nabla^\mu \varphi - V(\varphi) \right] + S_m(\psi^{(i)}, \tilde{g}_{\mu\nu}) \quad \tilde{g}_{\mu\nu} = A^2(\varphi) g_{\mu\nu}$$

Scalar Fifth Force

$$\ddot{\chi} + 2H\dot{\chi} + \frac{1}{a^2} \nabla(\Phi + \log A) = 0$$

$$\mathbf{F}_{\text{Fifth}} = -\frac{m}{a^2} \nabla \log A$$

$$\lambda_{\text{Fifth}} = \left(\frac{d^2 V_{\text{eff}}}{d\varphi^2} \right)^{-1/2}$$

$$V_{\text{eff}}(\varphi) = V(\varphi) + \rho_m [A(\varphi) - 1]$$

Hu-Sawicki Gravity

Hu & Sawicki (2007)

$$f(R) = -m^2 \frac{c_1 \left(\frac{R}{m^2}\right)^n}{c_2 \left(\frac{R}{m^2}\right)^n + 1}$$

$$V(\varphi) = \frac{m_{Pl}^2}{2} \frac{f_R R - f}{(1 + f_R)^2}$$

$$A(\varphi) = e^{\beta\varphi/m_{Pl}}$$

$$\lambda_{\text{Fifth}} = \frac{\sqrt{|f_{R0}|(n+1)}}{H_0} \left(\frac{\Omega_m + 4\Omega_\Lambda}{\Delta_m + 4\Omega_\Lambda} \right)^{1+\frac{n}{2}}$$

- Depends on f(R) parameters (f_{R0} , n) and local density of matter
- Screened in high density regions

N-body Simulations

Modified Poisson Equation (Jordan Frame)

$$\nabla^2 \Phi = \frac{16\pi G}{3} a^2 \delta\rho_m + \frac{a^2}{6} \delta R \quad \nabla^2 \delta f_R = -\frac{a^2}{3} [\delta R + 8\pi G \delta\rho_m]$$

Numerical Simulation Codes

- ECOSMOG Li, Zhao, Teyssier & Koyama (2012)

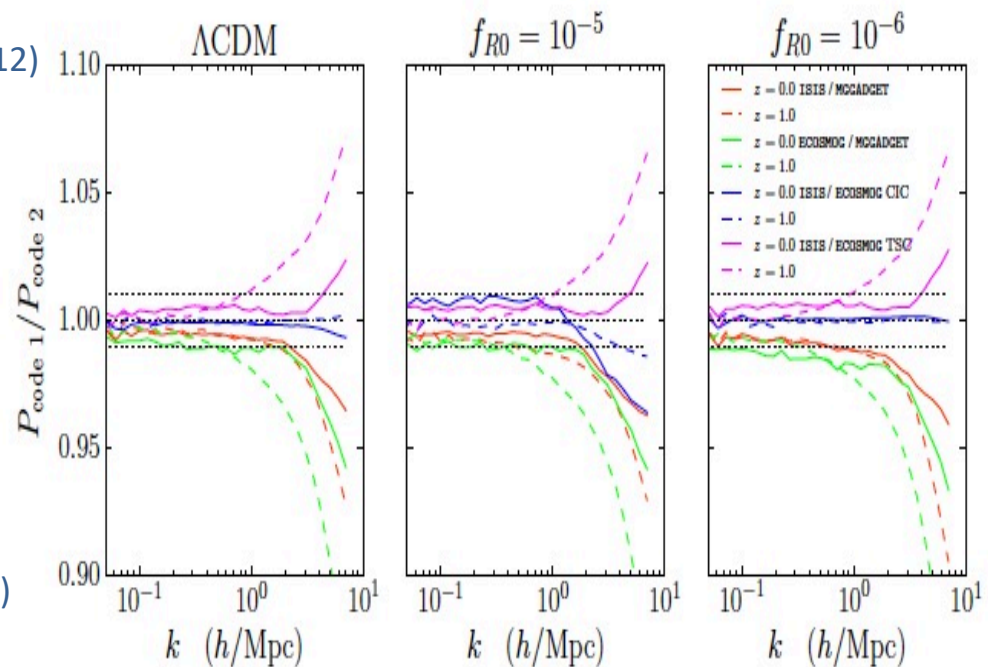
- Gravity Solver with AMR
- Based on RAMSES modification

- ISIS Linares, Mota & Winther (2013)

- Einstein Frame
- Poisson and φ Solver with AMR
- Based on RAMSES modification

- MG-Gadget Puchwein, Baldi, Springel (2013)

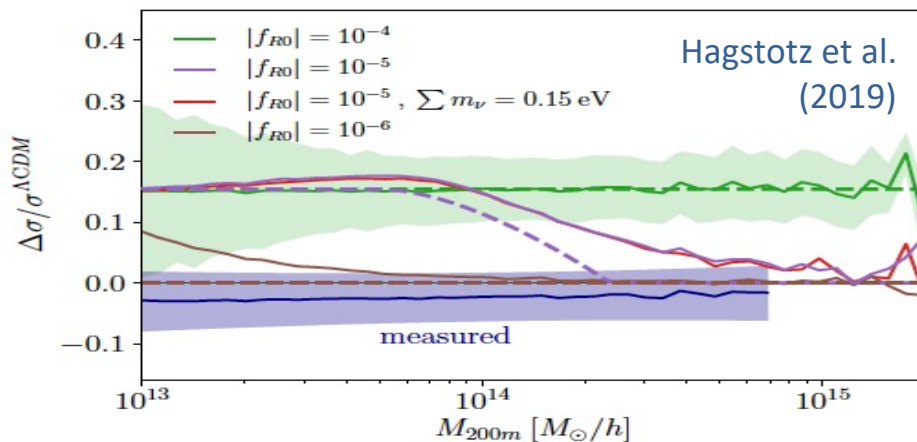
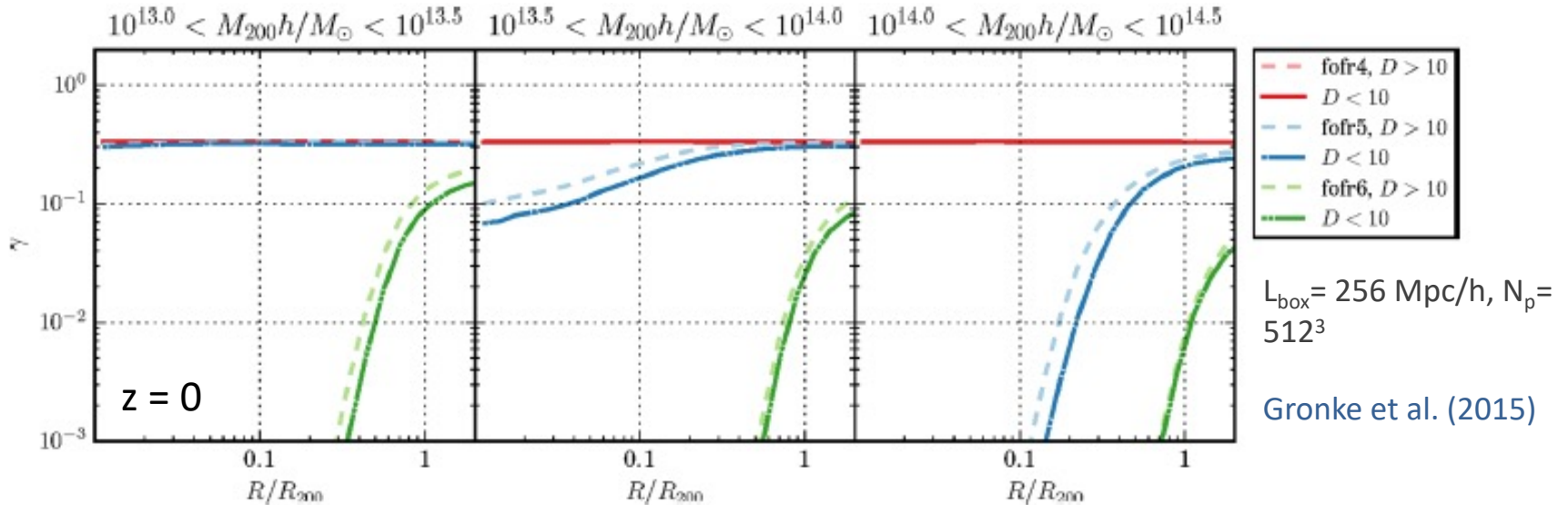
- Gravity Solver with TreePM
- Based on Gadget modification



Winther et al. (2015)

Unscreened Effects in Massive Halos

Scalar Fifth Force vs Newtonian Force



Enhanced Velocity Dispersion

- Dustgrain-Pathfinder Sims ($L_{\text{box}} = 750 \text{ Mpc}/h, N_p = 768^3$)
- Deeper Potential Well (unscreened regions)
- Virial Condition \rightarrow Higher Velocity Dispersion

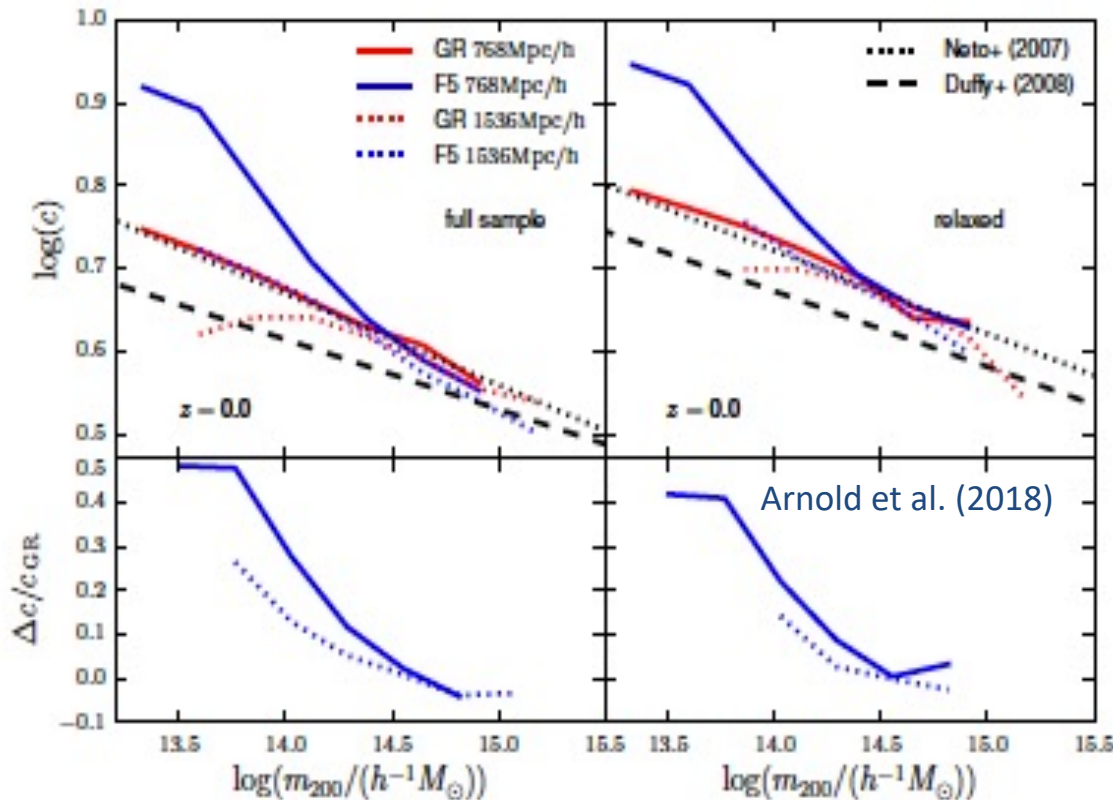
Halo Density Profiles

NFW Profile

$$\rho_{\text{NFW}}(r) = \frac{M_{200}}{4\pi[\ln(1+e) - e/(1+e)]} \times \frac{1}{r \left(\frac{r_{200}}{e} + r\right)^2} \quad c = \frac{r_{200}}{r_s}$$

halo concentration

Concentration-Mass Relation



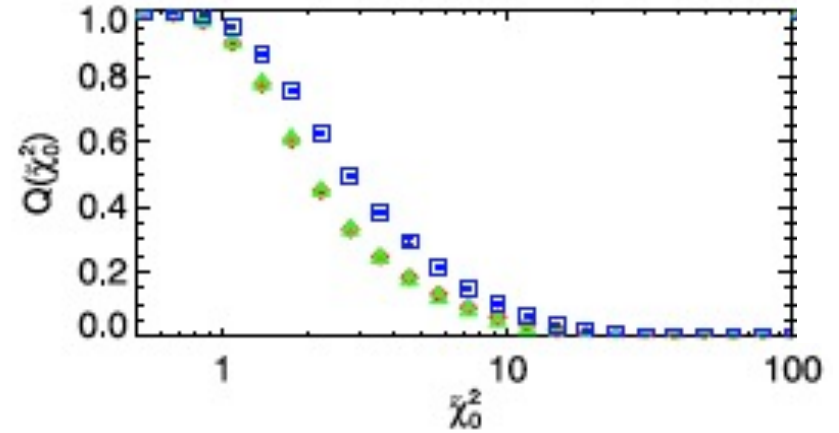
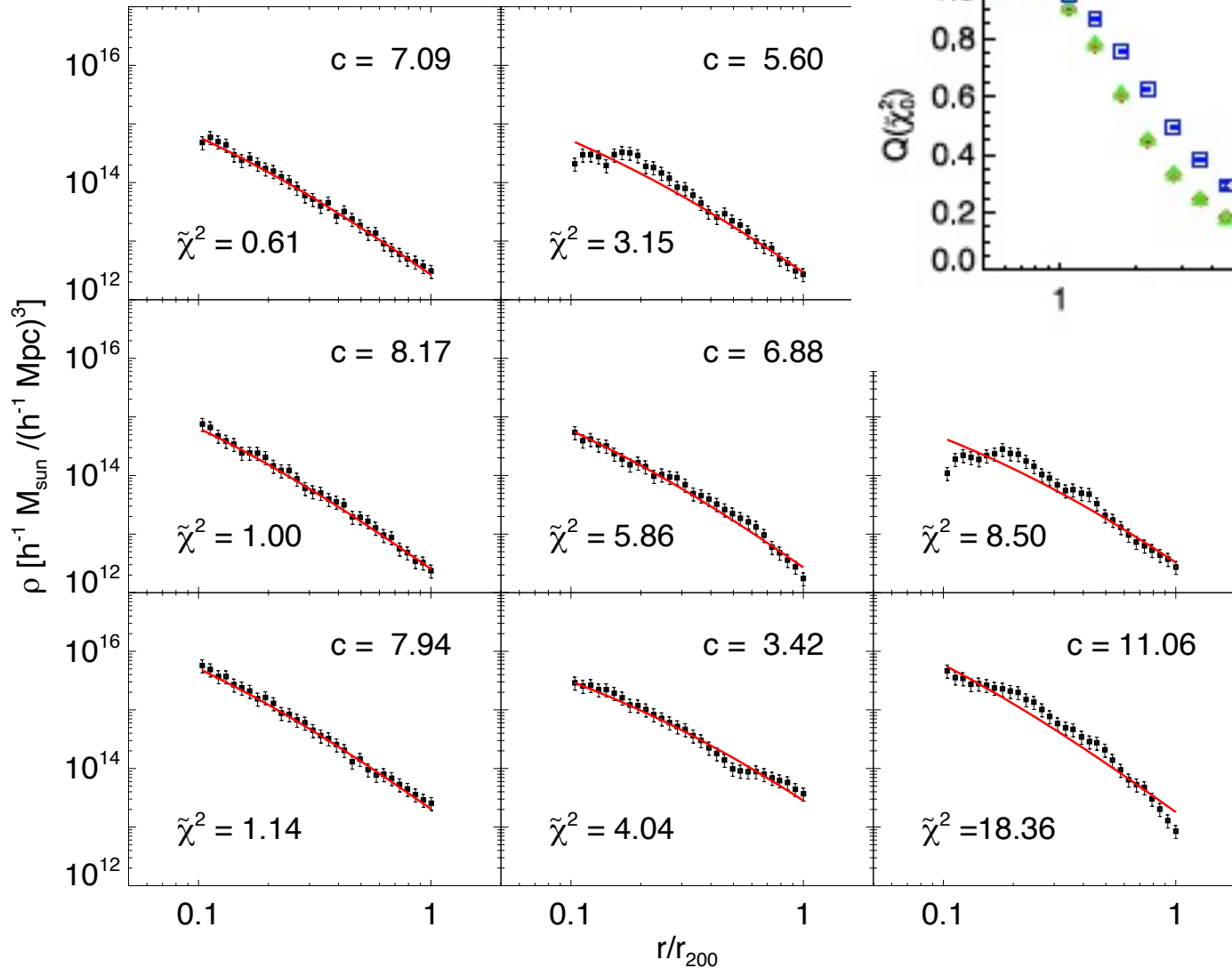
- $f(R)$ vs GR sims ($L_{\text{box}} = 768, 1536 \text{ Mpc/h}$, $N_p = 2048^3$)
- Unscreened halos are more concentrated

Pitfalls & Challenges

- Baryonic processes in the inner halo region e.g. Gnedin et al. (2004); Duffy et al. (2010); De Boni et al. (2013)
- Selection Effects and Observational Model Assumptions e.g. Oguri et al. (2005); Corless, King & Clowe (2009), Sereno et al. (2013)
- Goodness-of-fit of NFW to MG halos?
- Perturbed profiles

The Core of the Problem

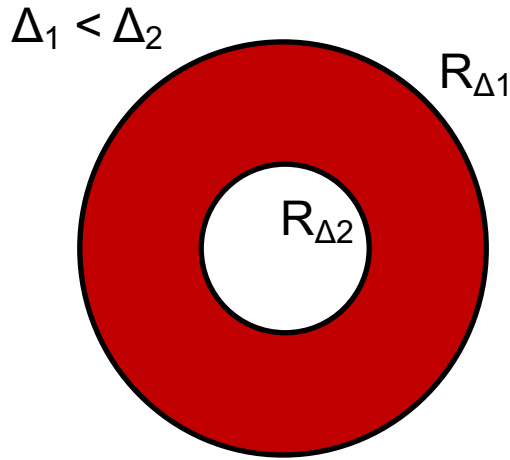
Balmes, Rasera, Corasaniti, Alimi (2014)



- distribution of c correlates with goodness-of-fit

See also Ragagnin et al. (2020)

Halo Sparsity



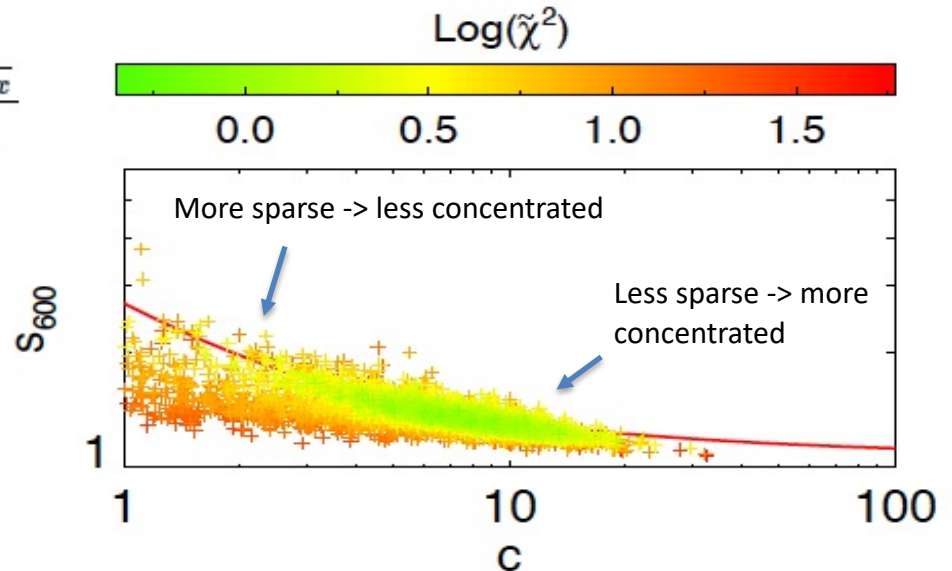
Mass Ratio $s_{\Delta_1 \Delta_2} = \frac{M_{\Delta_1}}{M_{\Delta_2}} \equiv 1 + \frac{\Delta M}{M_{\Delta_2}}$

- $\Delta_1 \geq 100$ (preserve halo individuality)
- $\Delta_2 \leq 2000$ (avoid baryon dominated region)

Sparsity of NFW Halos

$$s_{\Delta} = \frac{200}{x^3 \Delta} \quad \& \quad x^3 \frac{\Delta}{200} = \frac{\ln(1 + cx) - \frac{cx}{1+cx}}{\ln(1 + c) - \frac{c}{1+c}}$$

- Halos with $<1\sigma$ NFW along the expected relation
- Distributed nearly constant value with small scatter



Cosmological Proxy

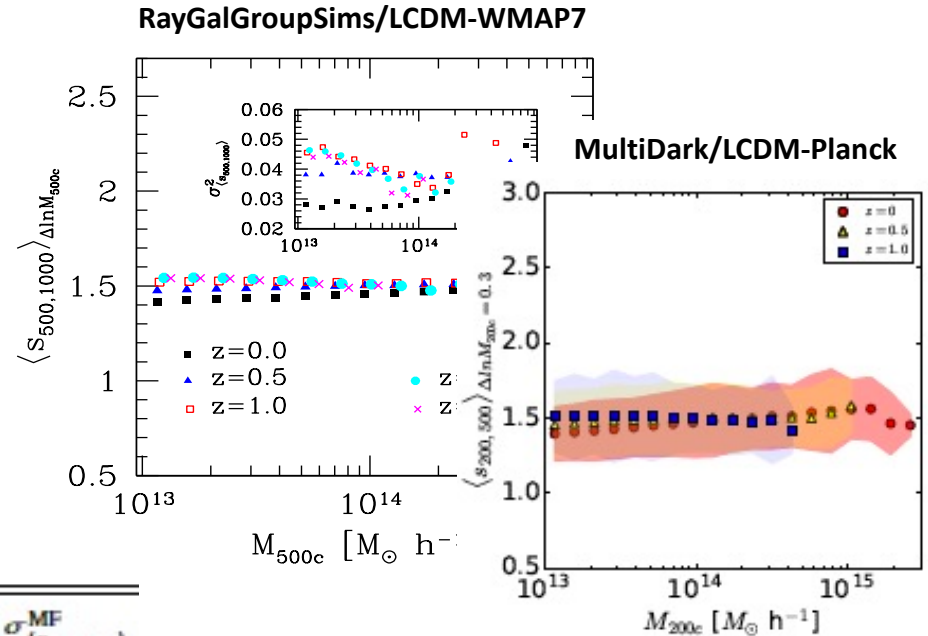
Halo Sparsity Properties Balmes et al. (2014); Corasaniti et al. (2018); Corasaniti & Rasera (2019)

- Nearly constant with mass (<10% variation across 2 orders in mass)
- Intrinsic scatter bounded to ~20%
- Trend independent of Δ_1 and Δ_2
- Average Sparsity from Halo Mass Function Relation

$$\int_{M_{\Delta_2}^{\min}}^{M_{\Delta_2}^{\max}} \frac{dn}{dM_{\Delta_2}} d\ln M_{\Delta_2} = \langle s_{\Delta_1, \Delta_2} \rangle \int_{\langle s_{\Delta_1, \Delta_2} \rangle M_{\Delta_2}^{\min}}^{\langle s_{\Delta_1, \Delta_2} \rangle M_{\Delta_2}^{\max}} \frac{dn}{dM_{\Delta_1}} d\ln M_{\Delta_1}$$

- Accurate to sub-percent level

| z | $\langle \frac{M_{200c}}{M_{500c}} \rangle$ | $\langle \frac{1/M_{500c}}{1/M_{200c}} \rangle$ | $\langle \frac{M_{200c}}{M_{500c}} \rangle$ | $\langle s_{200,500}^{MF} \rangle \pm \sigma_{(s_{200,500}^{MF})}$ | |
|--------|---|---|---|--|-----------------|
| MDPL2 | 0.0 | 1.42 | 1.41 | 1.42 | 1.40 ± 0.01 |
| | 0.5 | 1.47 | 1.46 | 1.46 | 1.48 ± 0.02 |
| | 1.0 | 1.51 | 1.51 | 1.48 | 1.52 ± 0.03 |
| Raygal | 0.0 | 1.50 | 1.48 | 1.49 | 1.49 ± 0.03 |
| | 0.5 | 1.54 | 1.53 | 1.53 | 1.54 ± 0.05 |
| | 1.0 | 1.55 | 1.54 | 1.52 | 1.54 ± 0.05 |



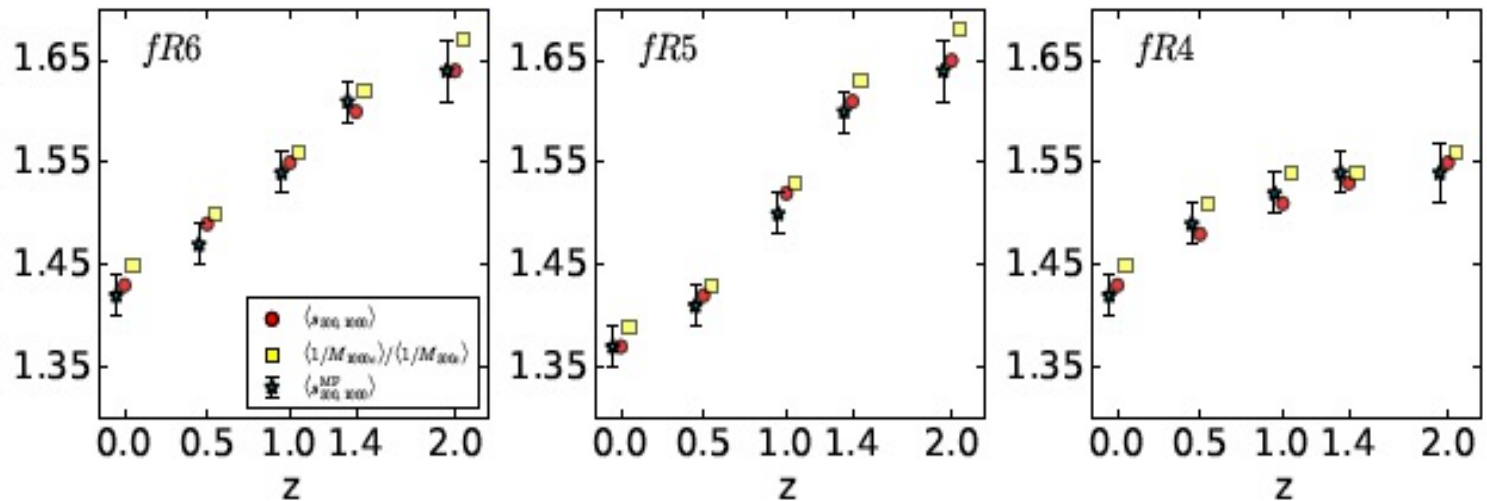
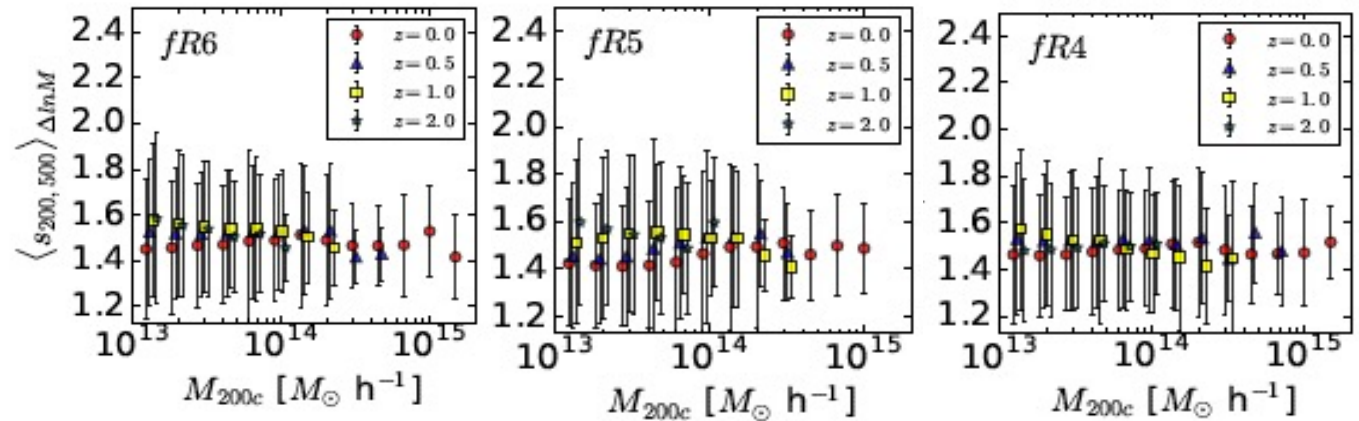
Consistency Relations

$$\langle s_{\Delta_1, \Delta_2} \rangle \equiv \left\langle \frac{M_{\Delta_1}}{M_{\Delta_2}} \right\rangle \cong \left\langle \frac{1/M_{\Delta_2}}{1/M_{\Delta_1}} \right\rangle \cong \langle s_{\Delta_1, \Delta_2}^{MF} \rangle$$

Halo Sparsity of f(R) models

Dustgrain-Pathfinder Halo Catalogs

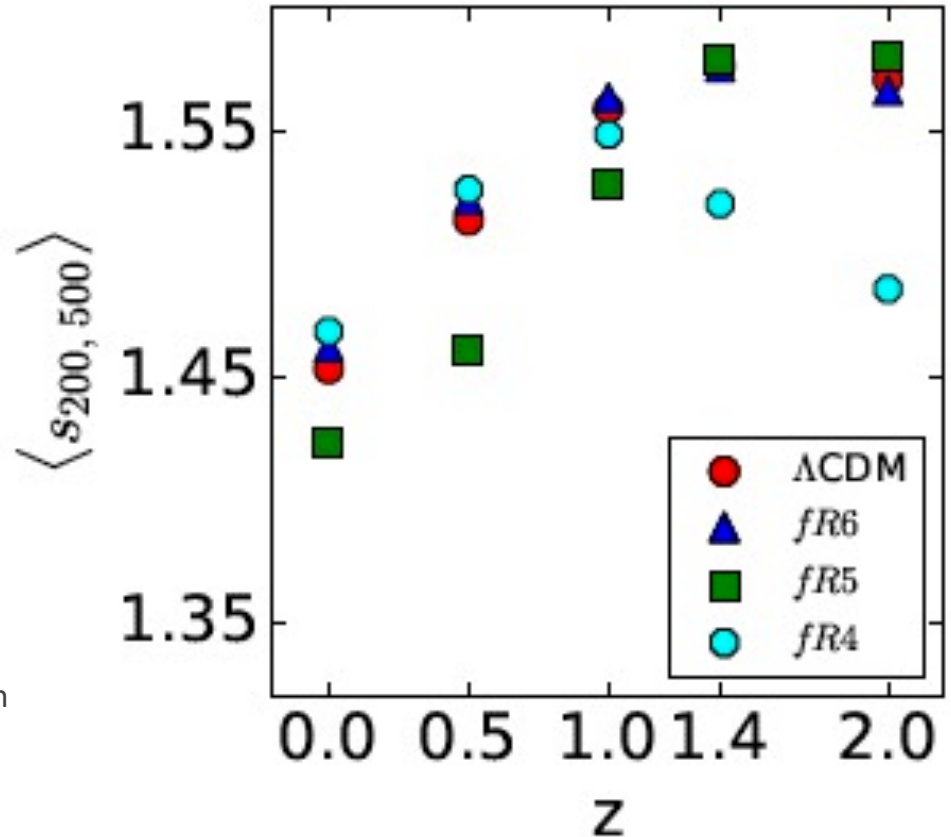
- SOD halos with $M_{200c} > 10^{13} M_{\text{sun}}/h$
- Independence with halo mass
- Consistency Relations



Screening Effects on Sparsity Evolution

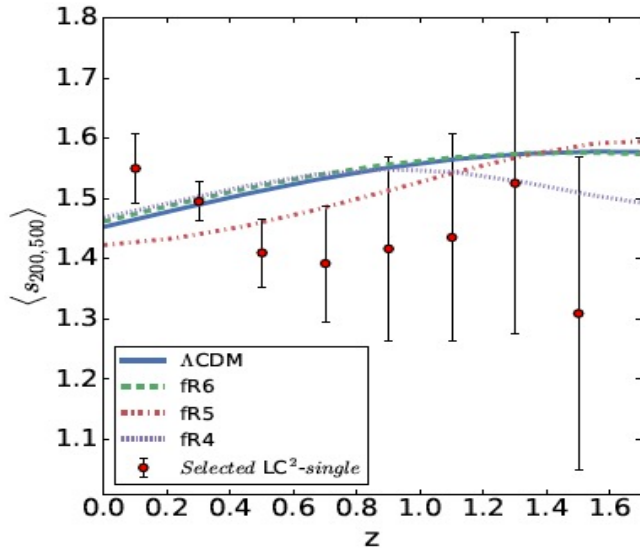
Ensemble Average Sparsity

- $|f_0| = 10^{-4}$: halos $> 10^{13} M_{\text{sun}}/h$ unscreened at $z = 0$
 - Linear Growth Enhanced than LCDM
 - Earlier Halo Formation -> More concentrated -> Less sparse
 - At $z < 1$, fifth force equally enhance radial profile of halos ($\langle s \rangle \sim \text{LCDM}$)
- $|f_0| = 10^{-5}$: halos $\sim 10^{13} - 10^{14} M_{\text{sun}}$ unscreened
 - Linear Growth $\sim \text{LCDM}$ ($\langle s \rangle \sim \text{LCDM}$)
 - Bulk of halos forming at $z < 1$ are unscreened in the inner region with enhanced halo profile (more concentrated -> less sparse)



- $|f_0| = 10^{-6}$: halos $\sim 10^{13} - 10^{15} M_{\text{sun}}$ screened
 - Sparsity evolution similar to LCDM

Observational Constraints



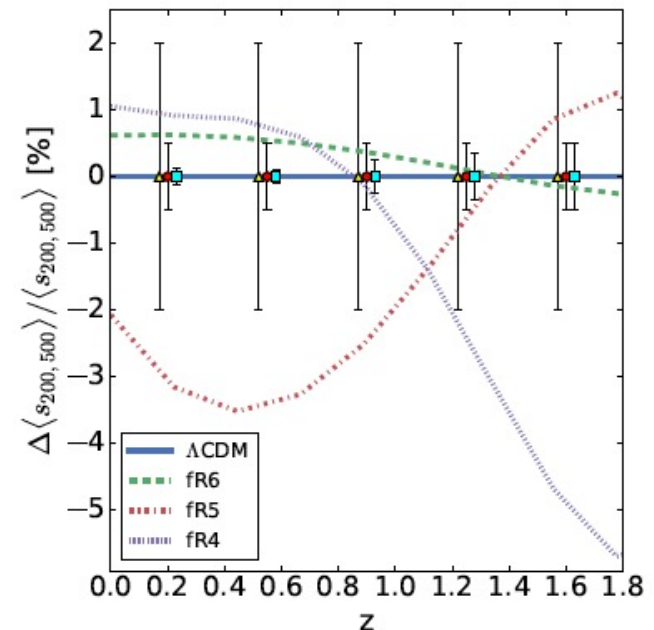
Cluster Lensing Masses

- Selected LC²-single cluster masses: 187 clusters
- No propagation of cosmological parameter degeneracies
- $\chi^2_{\Lambda\text{CDM}}=10.1$; $\chi^2_{fR6}=10.6$; $\chi^2_{fR5}=11.1$; $\chi^2_{fR4}=9.9$

Cluster Survey Forecast

- Uncertainty dominated by cluster mass errors
- Assuming $N \sim 1000$ clusters with $e_M = 30\%$, 5% , $\sim 1\%$ (*Euclid-like*)
- Systematics $\sim 2\%$ from radial dependent mass bias due to baryonic process (in LCDM)
- Dynamical Masses vs Lensing Masses

$$\Delta_M = \frac{d}{dr}(\Phi - \Psi) / \frac{d}{dr}(\Phi + \Psi)$$



Conclusions

- Unscreened scalar fifth force alters halo dynamical properties and mass distribution
- Depending on MG models enhanced velocity dispersion profile in group and cluster-like halos
- Modification in the halo mass distribution leads to testable predictions on the average halo sparsity evolution
- Needs of accurate cluster masses

Systematic Effects

Radial Dependent Mass Bias

- Baryonic Processes Altering Halo Mass Distribution (AGN feedback)

Velliscig et al. (2014)

- Hydrostatic Mass Bias

Biffi et al. (2016)

- Tangential Shear Profile

Becker & Kravtsov (2011)

| Cluster State | $r_{500,1000}$ [%] |
|---------------|--------------------|
| CC | -3.7 |
| NCC | 0.1 |
| Regular | 0.3 |
| Disturbed | -2.0 |

$$\frac{\Delta s_{\Delta_1, \Delta_2}}{s_{\Delta_1, \Delta_2}} = \frac{1 + y_{\Delta_1}}{1 + y_{\Delta_2}} - 1$$

